HHS Public Access

Author manuscript

Mol Psychiatry. Author manuscript; available in PMC 2016 August 02.

Published in final edited form as:

Mol Psychiatry. 2016 July ; 21(7): 956–968. doi:10.1038/mp.2015.222.

Maternal Immune Activation Leads to Selective Functional Deficits in Offspring Parvalbumin Interneurons

Sarah Canetta[1], **Scott Bolkan**[1], **Nancy Padilla-Coreano**[1,5], **LouJin Song**[2], **Ryan Sahn**, **Neil Harrison**[2,3], **Joshua A. Gordon**[1,5], **Alan Brown**[1,4,7], and **Christoph Kellendonk**[1,2,6]

[1]Department of Psychiatry, Mailman School of Public Health, Columbia University Medical Center, New York, NY 10032, USA

[2]Department of Pharmacology, Mailman School of Public Health, Columbia University Medical Center, New York, NY 10032, USA

[3]Department of Anesthesiology, Mailman School of Public Health, Columbia University Medical Center, New York, NY 10032, USA

[4]Department of Epidemiology, Mailman School of Public Health, Columbia University Medical Center, New York, NY 10032, USA

[5]Division of Integrative Neuroscience, New York State Psychiatric Institute, New York, NY 10032, USA

[6]Division of Molecular Therapeutics, New York State Psychiatric Institute, New York, NY 10032, USA

[7]Divison of Epidemiology, New York State Psychiatric Institute, New York, NY 10032, USA

Summary

Abnormalities in prefrontal GABAergic transmission, particularly in fast-spiking interneurons that express parvalbumin (PV), are hypothesized to contribute to the pathophysiology of multiple psychiatric disorders including schizophrenia, bipolar disorder, anxiety disorders and depression. While primarily histological abnormalities have been observed in patients and in animal models of psychiatric disease, evidence for abnormalities in functional neurotransmission at the level of specific interneuron populations has been lacking in animal models and is difficult to establish in human patients. Using an animal model of a psychiatric disease risk factor, prenatal maternal immune activation (MIA), we found reduced functional GABAergic transmission in the medial prefrontal cortex (mPFC) of adult MIA offspring. Decreased transmission was selective for interneurons expressing PV, and was not observed in calretinin-expressing neurons. This deficit in PV function in MIA offspring was associated with increased anxiety-like behavior and

Corresponding Author: Christoph Kellendonk, ck491@cumc.columbia.edu.

Conflict of Interest: The authors declare no conflict of interest.

Author Contributions

SEC, SB, AB, NH, JG and CK designed the experiments and wrote the manuscript. SEC, SB, NP, LS and RS performed the experiments.

impairments in attentional set shifting, but did not affect working memory. Furthermore, cell-type specific optogenetic inhibition of mPFC PV interneurons was sufficient to impair attentional set shifting and enhance anxiety levels. Finally, we found that *in vivo* mPFC gamma oscillations, which are supported by PV interneuron function, were linearly correlated with the degree of anxiety displayed in adult mice, and that this correlation was disrupted in MIA offspring. These results demonstrate a selective functional vulnerability of PV interneurons to maternal immune activation, leading to affective and cognitive symptoms that have high relevance for schizophrenia and other psychiatric disorders.

Introduction

Abnormalities in prefrontal cortical gamma amino butyric acid (GABA)-ergic interneurons are hypothesized to be integral to the pathophysiology of several psychiatric disorders, including schizophrenia, bipolar disorder, anxiety disorder and depression[1-16]. This hypothesis is based on post-mortem histological findings and *in vivo* imaging results. In schizophrenia, mRNA and protein reductions in glutamate decarboxylase 67 (GAD67), an enzyme responsible for the synthesis of GABA, have been consistently identified in layer 3 of the prefrontal cortex (PFC)[9-11, 17-19]. Alterations in other GABAergic markers have also been shown, including the GABA transporter, vGAT1 and the GABA receptor subunits, $GABA_A\alpha1$, α2 and δ[17-21]. Furthermore, *in vivo* brain imaging studies have found alterations in prefrontal GABA levels and $GABA_A$ receptor binding in schizophrenia[13, 22]. While less well-studied, histological alterations in GABAergic markers as well as reductions in prefrontal GABA and $GABA_A$ receptor binding have also been reported in other psychiatric disorders including bipolar disorder, depression and anxiety disorder[1-2, 4-8, 14-16].

GABAergic interneurons show a remarkable diversity of both form and function, and a variety of populations can be distinguished histologically based on their expression of molecular markers[23-25]. In schizophrenia, substantial interest has focused on a population of interneurons that express the marker parvalbumin (PV) because histological and protein expression abnormalities are most frequently seen in this interneuron population[10, 19, 26-27]. Similar reductions in PV have also been observed in bipolar disorder and depression, while PV changes in anxiety disorder remain unexplored[1, 28-29]. PV interneurons have generated high interest as they are essential for the production of cortical oscillations in the gamma frequency (30-80 Hz), a physiological measure of brain function that is thought to support cognitive processes including working memory and attentional set shifting[30-37]. In contrast, histological alterations have not been seen in a separate population of interneurons that express the molecular marker, calretinin (CR)[10, 17, 19, 38-40]. Despite this extensive evidence documenting abnormalities in the prefrontal GABAergic system, and in particular in PV interneurons, it remains unclear whether the histological and imaging alterations reflect *functional* changes in prefrontal GABAergic transmission, and if so, which populations of interneurons are affected.

Our ability to assess the function of prefrontal GABAergic interneurons, particularly at the level of individual interneuron subpopulations, is limited in humans. Moreover, in humans it is nearly impossible to causally relate cell-type-specific dysfunction to behavioral

symptoms. Animal models of genetic or environmental risk factors for psychiatric disorders provide a complementary approach to assay functional changes in specific types of prefrontal cortical GABAergic interneurons, as well as their relevance to behavior.

Here, we have chosen to model an environmental exposure, prenatal infection and subsequent maternal immune activation (MIA), because substantial epidemiological evidence supports MIA as a risk factor for the *in utero* offspring later developing psychopathology. Associations between MIA and offspring risk of schizophrenia and bipolar disorder have been found in prospective birth cohort studies, including those that used archived maternal serum samples during the pregnancy to serologically validate infection status[41-43]. Preliminary associations, based on retrospective data or ecological studies, have also been reported between MIA and depression and anxiety disorder[44-45]. As MIA is a common exposure, findings from this model will be relevant to a considerable proportion of people with these illnesses[41]. MIA can be modeled with high construct validity in mice by infecting pregnant dams with live virus or by activating the maternal immune system via injection of double-stranded RNA (Poly IC)[46]. Importantly, histological abnormalities in GABAergic markers in the mPFC have already been reported in adult MIA offspring, although effects on functional GABAergic transmission have never been assayed *in vitro* or *in vivo* at the level of specific interneuron populations[47]. We therefore used a murine MIA model, in combination with electrophysiological studies, to investigate whether prenatal MIA affects the *functioning* of prefrontal GABAergic interneurons in adult offspring.

We found that pyramidal cells in layer 2/3 of the mPFC of adult MIA offspring receive reduced GABAergic transmission. Using optogenetic tools in combination with cell-type-specific gene targeting, we found that functional inhibitory transmission between PV interneurons and pyramidal cells was dramatically reduced, whereas transmission from calretinin (CR) and somatostatin (SST) containing interneurons was not altered.

Since cortical interneuron function has been implicated in regulating cognitive processes, as well as affective behaviors, we assessed MIA offspring in tasks addressing these behaviors. Adult MIA offspring displayed deficits in attentional set shifting, but did not reveal any impairment in two independent working memory tasks. Additionally, we found that adult MIA offspring displayed increased anxiety-like behavior. Intriguingly, optogenetic inhibition of prefrontal PV interneuron function was sufficient to recapitulate both the deficit in attentional set shifting and the increase in anxiety-like behavior seen in adult MIA offspring. PV interneurons are essential for gamma oscillations[32, 34], and prefrontal gamma oscillations have been shown to support attentional set shifting behavior[37], although a role in anxiety-related behaviors has not been explored. Therefore, we measured oscillatory activity within the prefrontal cortex in mice performing an anxiety-related task, the elevated plus maze (EPM). We found that cortical gamma power was correlated with anxiety-like behavior in the EPM and this relationship was disrupted in MIA offspring. Our results indicate a selective vulnerability of the PV class of inhibitory interneurons to maternal immune activation leading to impairments in set shifting and enhanced anxiety levels via disruption of high-frequency neuronal activity.

Materials and Methods

A brief summary of experimental procedures is provided here with additional details available in the Supplemental Information accompanying this article. Additionally, Supplementary Table 1 provides an overview of the number of animals used for the various experiments; for comparisons of MIA and Saline offspring, the number of litters used to generate the experimental mice is also included.

Animal Husbandry

All animal procedures were approved by Columbia University's Animal Care and Use Committee. C57/bl6 (Jackson Labs, Stock #000664) matings were used to produce offspring for mIPSC and sIPSC physiology, histology, animal behavior and cytokine analyses. Parvalbumin Cre (PV-Cre, Jackson Stock #008069), Calretinin Cre (CR-Cre, Jackson Labs, Stock #010774) or Somatostatin Cre (SST-Cre, Jackson Labs, Stock #013044) males were bred with homozygous Floxed-Stop-ChannelRhodopsin2-YFP (Jackson Labs, Stock #012569) females to produce offspring that were used for optogenetic electophysiology experiments. Adult (8-12 week old) PV Cre mice were used for viral injections (bilateral injection of 0.4 μl of AAV5-DIO-ef1α-eArch3.0 or AAV5-DIO-hSYN-GFP, UNC Vector Core) and implantation with optic fibers (0.22 NA) for *in vivo* optogenetic behavioral experiments. Animals were allowed to recover for 5 weeks prior to behavioral testing. Animals were fed ad libitum and reared under normal lighting conditions (12/12 light/dark cycle), unless otherwise noted. Adult (P90-110) male and female MIA and Saline offspring were used for electrophysiology experiments (no effects of gender were seen); Adult (> P90) male mice were used for behavior and histology. A subset of adult male MIA and Saline offspring that completed behavioral testing were subsequently used for *in vivo* local field potential (LFP) recordings. An additional group of 12 adult male 129 SvEvTac (Taconic) mice were used for LFP recordings correlating gamma and open arm time.

Drugs

Polyinosinic-Polycytidylic acid (Poly IC; Sigma-Aldrich; P9582) was prepared as a stock solution of 0.5 mg/mL (calculated based on the weight of Poly IC alone). Pregnant dams bearing embryos received either an intravenous injection of 1 mg/kg Poly IC or vehicle (physiological Saline) solution on embryonic day 9 (E9). For electrophysiology, 20 μM 6-cyano-7-nitroquinoxaline-2,3-dione disodium salt (CNQX, Tocris Bioscience), 50 μM D-(-)-2-Amino-5-phosphonopentanoic acid (AP5, Tocris Bioscience), 2 μM tetrodotoxin citrate (TTX, Tocris Bioscience) and 10 μM (-)-bicuculline methiodide (Tocris Bioscience) were added to the perfusate where noted.

Cytokine Assay

Cytokines (IL-6 and TNFα) were measured using Milliplex MAP Mouse cytokine/chemokine assay (Invitrogen) on a Luminex System (Luminex Corp) from the serum collected from pregnant dams 3 hours following intravenous injection of Poly IC (1, 2.5 or 5 mg/kg) or Saline on embryonic day 9 (e9).

Electrophysiology

Whole-cell current and voltage clamp recordings were performed in layer 2/3 pyramidal cells and fast-spiking PV-expressing interneurons in the prelimbic (PrL) region of the mPFC. Recordings were obtained with a Multiclamp 700B amplifier (Molecular Devices) and digitized using a Digidata 1440A acquisition system (Molecular Devices) with Clampex 10 (Molecular Devices) and analyzed with pClamp 10 (Molecular Devices). Following decapitation, 300 μM slices containing mPFC were incubated in artificial cerebral spinal fluid (ACSF) containing (in mM) 126 NaCl, 2.5 KCl, 2.0 $MgCl_2$, 1.25 NaH_2PO_4, 2.0 $CaCl_2$, 26.2 $NaHCO_3$ and 10.0 D-Glucose, bubbled with oxygen, at 32° C for 30 minutes before being returned to room temperature for at least 30 minutes prior to use. During recording, slices were perfused in ACSF (with drugs added as detailed below) at a rate of 5 mL/minute. Electrodes were pulled from 1.5 mm borosilicate-glass pipettes on a P-97 puller (Sutter Instruments). Electrode resistance was typically 3–5 MΩ when filled with internal solution consisting of (in mM): 130 K-Gluconate, 5 NaCl, 10 HEPES, 0.5 EGTA, 2 Mg-ATP, and 0.3 Na-GTP (pH 7.3, 280 mOsm).

mIPSC and sIPSC Recordings

Pyramidal cells were visually identified based on their shape and prominent apical dendrite at 40x magnification under infrared and diffusion interference contrast microscopy using an inverted Olympus BX51W1 microscope coupled to a Hamamatsu C8484 camera. sIPSCs were recorded in voltage clamp at a holding potential of −70 mV using an intracellular solution containing (in mM): 136.5 KCl, 10 HEPES, 0.5 EGTA, 2.0 MgATP and 0.3 NaGTP (pH 7.3, 280 mOsm). 20 μM CNQX and 50 μM AP5 were added to the bath to block glutamatergic currents. 60 seconds of the current recording was filtered with an eight-pole low-pass Bessel filter and sIPSCs were detected using MiniAnalysis (Synaptosoft). Events with an amplitude greater than five times the root mean square (RMS) baseline noise were included; all event data was averaged by cell. mIPSCs were recorded and analyzed as above but 2 μM TTX was added to the bath during recording. 10 μM bicuculline methiodide was added to the bath to verify the m/sIPSCs were $GABA_A$-mediated.

Optogenetic Stimulation Experiments

Pyramidal cells were visually identified based on their shape and prominent apical dendrite at 40x magnification under infrared and diffusion interference contrast microscopy using an inverted Olympus BX51W1 microscope coupled to a Hamamatsu C8484 camera. The recorded cell was placed in the center of the field of view, held at −70 mV in voltage clamp and the response to a current evoked by a 5-ms pulse of blue light (470 nm) applied by a light emitting diode (LED, Cool LED) was recorded. The intensity of the LED was set at 5% of maximum intensity. The current trace was filtered with an eight-pole low-pass Bessel filter and the difference between the baseline and the maximum light-evoked current response was recorded. If the magnitude of the response was greater than 2 times the root mean square (RMS) noise, it was considered a significant response. For presynaptic release probability experiments, four 5-ms pulses of the LED at 5% maximum intensity were applied at a frequency of 20 Hz and the response to each of the pulses was analyzed as above.

***In vivo* Optogenetic Behavior—**Lasers emitting green light (532 nm) at 10 mW were connected via patchcords to a rotary joint that was then connected via patchcords (200 μm, 0.22 NA) to the light fibers implanted in the animal's head to activate eArch3.0. Mice were randomized to receive light ON or OFF in a counter-balanced fashion.

***In vivo* Neurophysiology—**A subset of adult male MIA and Saline offspring used for behavioral testing were subsequently unilaterally implanted with a 75 μm tungsten electrode in the PrL region of the mPFC (AP +1.8, ML + 0.3, DV −1.8) that was cemented directly to the skull during surgery and attached to a 16-channel electronic interface board (EIB-16, Neuralynx, Bozeman, MT). *In vivo* LFP recordings were performed while the animals were in the elevated plus maze. Recordings were obtained via a unitary gain head-stage preamplifier (HS-16; Neuralynx) attached to a fine wire cable. Field potential signals from the mPFC were recorded against a screw implanted in the anterior portion of the skull. LFPs were amplified, bandpass filtered (1–1,000 Hz) and acquired at 2000 Hz. LFP data was acquired with Lynx 8 programmable amplifiers on a personal computer running Cheetah data acquisition software (Neuralynx). The animal's position was obtained by overhead video tracking (30 Hz) of a light-emitting diode affixed to the head stage.

LFP data was imported into Matlab using custom-written software. Gamma power was calculated using the Welch's modified method of spectral estimation (*pwelch*, Matlab) using a 1 s sliding window of 90% overlap, using 4000 fast Fourier transformations (nFFT). Mean gamma was calculated for the canonical range of 30-80 Hz. Mean gamma and open arm time was calculated for 10 minutes in the EPM for Saline and MIA mice and 129 SvEvTac mice. Electrode locations were confirmed to be within the PrL PFC based on location of electrolytic lesions.

Histology—Adult mice were perfused with phosphate buffered saline (PBS) followed by 4% paraformaldehyde (PFA) in PBS and the brains were post-fixed in 4% PFA overnight. Brains were sectioned serially at 50 μm on a vibratome (Leica). The following primary antibodies were used: Parvalbumin (PV, Sigma, P3088, 1:2000 or abcam, ab13970, 1:1000), Glutamate Decarboxylase 65 (GAD65, Millipore, MAB351, 1:1000), Glutamate Decarboxylase 67 (GAD67, Millipore, MAB5406, 1:500), Microtubule-associated Protein (MAP2, Abcam, ab5392, 1:5000), Calretinin (CR, Swant, 7699/3H, 1:2000), Somatostatin (SST, Millipore, mab354, 1:250), Vasoactive Intestinal Peptide (VIP, Immunostar, 20077, 1:250) or green fluorescent protein (GFP, Life Technologies, A10262, 1:1000). Alexa Fluor-conjugated secondary antibodies (Invitrogen, 1:1000) were used for used for secondary detection. Stereology was used to assess PV cell number in the PrL region of adult MIA and Saline offspring using StereoInvestigator software (MBF Biosciences). PV and GAD65 perisomatic puncta as well as levels of GAD67 present in PV-expressing cells in the PrL region of MIA and Saline offspring were estimated from analysis of 40x confocal images of sections stained for either PV and MAP2, GAD65 and MAP2 or GAD67 and PV, using Image J software. During image acquisition and quantification, the investigator was blind to the treatment.

Behavior—MIA and Saline offspring were compared on the Elevated Plus Maze, Open Field, Attentional Set Shifting Task, Delayed Alternation Operant Task and the Delayed

Non-Match to Sample T-maze. Optogenetic experiments were performed in the Elevated Plus Maze and Attentional Set Shifting Task. Neurophysiology experiments were performed in the Elevated Plus Maze.

Statistical Analysis—Data were analyzed using Prism (GraphPad). For comparison of 2 groups, two-tailed Student's t-tests were used where the data was normally distributed and Mann-Whitney tests were used where the data was not normally distributed. We assessed the variance between groups and if it was unequal, a statistical correction was applied. For comparison of categorical data, a Fisher's exact test was used. For comparison of repeated measurements, >2 groups, or multiple variables, 1 or 2-way ANOVA was used if the data was normally distributed and a Kruskill Wallis test was used if it was not. Power analyses were conducted to estimate sample sizes. In the text, data are reported as the mean±standard error of the mean. Box and whisker plots depict the median with a line, the first and the third quartiles with the ends of the box and the maximum and minimum at the ends of the whiskers. Bar graphs depict the mean±standard error of the mean.

Results

Animal models of maternal immune activation (MIA) differ in the dose of Poly IC delivered, the route of administration, and the time during pregnancy when the drug is administered. We chose to deliver the drug on embryonic day 9 (e9) of a mouse pregnancy because this is analogous to the late first/early second trimester period in a human pregnancy, which has been identified as a window of increased vulnerability to the effects of infection in the developing offspring in the human epidemiological literature[41, 48]. Based on our dose-response assay of the effects of intravenously administered 1, 2.5 and 5 mg/kg of Poly IC on maternal inflammatory cytokines 3 hours following injection, as well as on maternal and fetal outcomes, we selected 1 mg/kg as the optimal dose to robustly induce MIA in our animal facility (Table 1, comparable to levels reported in the literature[49]) while not grossly increasing maternal or fetal deaths (Table 2).

Prenatal MIA decreases inhibitory post-synaptic currents in mPFC pyramidal cells in adult offspring

To examine whether prenatal MIA affects functional GABAergic transmission in the mPFC of adult offspring, we performed whole-cell patch clamp recordings of spontaneous inhibitory post-synaptic currents (sIPSCs) from pyramidal cells in slices containing the PrL region of the mPFC. We found a reduction in both the frequency (Figure 1A, B; Saline, 3.70±0.84 Hz, n=17 cells from 7 animals; MIA, 1.56±0.29 Hz, n=18 cells from 5 animals; Mann Whitney test: $p<0.05$) and the amplitude (Figure 1A, B; Saline, 66.02±9.65 pA, n=17 cells from 7 animals; MIA, 40.53±3.42 pA, n=18 cells from 5 animals; Mann Whitney test: $p<0.01$) of sIPSCs in pyramidal cells from MIA offspring. To determine if this reduction in sIPSCs was the result of pre- or post-synaptic alterations, we recorded miniature inhibitory post-synaptic currents (mIPSCs) in the presence of tetrodotoxin (2 μM). Under these conditions, we found that the frequency (Figure 1 C, D; Saline, 1.08±0.16 Hz, n=15 cells from 4 animals; MIA, 0.64±0.10 Hz, n=15 cells from 3 animals; t-test: $p<0.05$), but not the amplitude (Figure 1C, D; Saline, 35.18±2.70 pA, n=15 cells from 4 animals; MIA,

33.96±2.43 pA, n=15 cells from 3 animals) of mIPSCs was reduced in pyramidal cells from MIA offspring, suggesting a pre-synaptic contribution to the loss of GABAergic transmission.

Prenatal MIA decreases GABAergic transmission between PV-expressing interneurons and pyramidal cells in the mPFC of adult offspring

Next, we sought to ascertain which interneuron population is responsible for the deficits in functional GABAergic transmission in MIA offspring. To measure functional GABAergic connectivity between different populations of prefrontal interneurons and their post-synaptic pyramidal cell targets, we selectively expressed the light-sensitive cation channel, Channelrhodopsin2 (ChR2) fused to YFP in PV, CR and SST-expressing prefrontal interneurons using timed matings between floxed ChR2 females and PV-Cre, CR-Cre or SST-Cre males. Pregnant females were injected on e9 with either 1 mg/kg of Poly IC or Saline, producing MIA and Saline offspring on a PV-ChR2, CR-ChR2 or SST-ChR2 background.

We verified the selectivity of the PV-Cre mouse by performing double immunohistochemistry for the ChR2-YFP fusion protein and PV. Virtually all (97%) of ChR2-YFP positive neurons co-expressed PV (Figure 2B and Supplementary Table S2). Pyramidal cells were patched in slices containing the PrL mPFC, held at −70 mV while a 5 ms pulse of blue light (470 nm) was applied to the field of view, and the resulting amplitude of the inhibitory light-evoked post-synaptic current (le-IPSC) was used as a proxy for PV-pyramidal cell functional connectivity. We confirmed the observed le-IPSC was mediated by GABA, as it was blocked by 20 μM bicuculline (Supplementary Figure S1A, B). We found that the amplitude of le-IPSCs evoked by stimulation of PV interneurons was significantly reduced in MIA offspring (Figure 2C, D; Saline, 58.30±6.71 pA, n=26 cells from 9 animals; MIA, 21.99±6.17 pA, n=37 cells from 10 animals; Mann Whitney test: $p<0.001$). Under our recording conditions, 100% of the pyramidal cells patched from our Saline offspring had a significant le-IPSC response (defined as a le-IPSC amplitude >2x the standard deviation of the baseline noise). However, only 63% of the pyramidal cells recorded from MIA offspring, had a significant le-IPSC (Figure 2E; Fisher's exact test: $p<0.001$). This loss of functional GABAergic transmission between PV and pyramidal cells in MIA offspring was not due to a decreased ability of ChR2 to activate PV interneurons in MIA offspring as light-evoked spiking in PV-ChR2 cells was comparable in MIA and Saline offspring (Figure 2F; Saline, 2.95±0.21 spikes, n=12 cells from 8 animals; MIA, 2.75±0.12 spikes, n=15 cells from 8 animals).

Prenatal MIA does not alter GABAergic transmission between CR and SST-expressing interneurons and pyramidal cells in the mPFC of adult offspring

To determine whether this change in functional connectivity was selective for PV interneurons, we measured le-PSCs in MIA and Saline offspring on a CR-ChR2 background. We first verified the selectivity of the CR-ChR2 mouse by performing double immunohistochemistry for the ChR2-YFP fusion protein and CR. Virtually all (92%) of ChR2 positive neurons co-expressed CR (Figure 2H and Supplementary Table S3). Due to the possibility of overlap between CR-ChR2 expressing neurons and SST or vasoactive

intestinal peptide (VIP) expression, we quantified the percentages of ChR2-expressing cells that express either SST or VIP in CR-ChR2 mice. We found no ChR2-expressing cells co-expressed SST although 36% of ChR2-expressing cells also expressed VIP (Supplementary Table S3). Using CR-ChR2 mice, the net le-PSC in pyramidal cells at a holding potential of −70 mV in response to 5 ms of blue light stimulation of CR interneurons was surprisingly excitatory, rather than inhibitory (Supplementary Figure S1C). This is likely due to dis-inhibition of other interneuron populations. Disinhibitory circuits have been described in PFC mediated by interneurons that express VIP[50]. These VIP interneurons primarily synapse onto SST interneurons, and, to a lesser extent, PV interneurons, resulting in a net disinhibition of pyramidal cells when VIP cells are activated[50]. While the local connectivity of CR interneurons has not been studied, we have found abundant overlap between somatic expression of CR-driven ChR2 and VIP, in-keeping with the results of prior studies[51-52]. Thus, by stimulating CR interneurons we may be activating the same disinhibitory circuit engaged by activation of a subpopulation of VIP cells.

Although the net effect of activating CR interneurons is to disinhibit pyramidal cells, it is possible to isolate inhibitory connections made by CR interneurons onto pyramidal cells by performing the CR stimulation experiments in the presence of 20 μM CNQX and 50 μM AP5 at a holding potential of −50 mV, to maximize the driving force on chloride. We confirmed that the observed le-IPSC under these conditions was mediated by GABA by blocking it with 20 μM bicuculline (Supplementary Figure S1 D, E). Unlike the PV interneurons, le-IPSCs from CR stimulation were equivalent in MIA and Saline offspring (Figure 2I, J; Saline, 82.82±11.18 pA, n=25 cells from 6 animals; MIA, 72.47±10.33 pA, n=22 cells from 4 animals). In both MIA and Saline offspring, 100% of the pyramidal cells tested displayed significant current responses (Figure 2K). We also confirmed that light stimulation evoked a comparable number of spikes in CR-ChR2 cells in MIA and Saline offspring (Figure 2L; Saline, 1.90±0.68 spikes, n=5 cells from 4 animals; MIA, 2.45±0.47 spikes, n=6 cells from 2 animals).

We also looked at light-evoked currents from SST cells, a third population distinct from PV-ChR2 and CR-ChR2 positive neurons, in a limited number of MIA and Saline offspring on a SST-ChR2 background. Similar to currents from PV-ChR2 cells, light evoked currents from SST-ChR2 cells were inhibitory at a holding potential of −70 mV, although the size of the light-evoked current from SST-ChR2 cells was smaller in amplitude. We did not detect a difference in the amplitude of light-evoked currents from SST-ChR2 cells between Saline and MIA offspring (Supplementary Figure S2B&C; Saline, 22.03 ± 4.359 pA, n=7 cells from 2 animals; MIA, 25.76 ± 13.48 pA, n=10 cells from 3 animals). As with PV and CR cells, light evoked comparable levels of spiking in SST cells in MIA and Saline offspring (Figure Supplementary Figure S2E; Saline, 2.67 ± 0.67 spikes, n=3 cells from 2 animals; MIA, 2.0 ± 0.0 spikes, n=1 cell from 1 animal). Thus, GABAergic transmission from PV, but not CR or SST, interneurons onto pyramidal cells in the mPFC is selectively decreased in MIA offspring.

Prenatal MIA decreases release probability at PV interneuron-pyramidal cell synapses in the mPFC of adult offspring

Decreases in functional transmission between PV interneurons and pyramidal cells could result from anatomical or physiological causes. To assess whether MIA offspring have less PrL mPFC PV interneurons, we conducted stereological counts of PV cells in that region from 8 Saline and 9 MIA offspring. We found no reduction in the total number of PV cells in MIA offspring (Supplementary Figure S3A; Saline, 1467±122 cells, n=8 animals; MIA, 1362±203 cells, n=9 animals) or in their cell density (Supplementary Figure S3B; Saline, 1.81±0.09 cells/counting frame, n=8 animals; MIA, 1.73±0.16 cells/counting frame, n=9 animals). Similarly, when we quantified inputs from PV interneurons to pyramidal cells by counting perisomatic puncta identified with either PV or the presynaptically enriched GABAergic marker, GAD65, we found no change in MIA offspring (Figure 3; PV Punctal Number: Saline, 7.52±1.78; MIA, 6.65±1.40; PV Puntal Size (μm^2): Saline, 0.47±0.03; MIA, 0.47±0.05; PV Punctal Intensity (A.U.): Saline, 853.2±18.8; MIA, 826.5±59.3; GAD65 Punctal Number: Saline, 8.25±0.99; MIA, 9.41±1.11; GAD65 Punctal Size (μm^2): Saline, 0.42±0.03; MIA, 0.43±0.03; GAD65 Punctal Intensity (A.U.): Saline, 1000.0±8.4; MIA, 999.5±15.5; n=8 Saline animals and 9 MIA animals). Cumulatively, these results suggest that the loss of GABAergic transmission from PV interneurons in MIA offspring is not the result of anatomical alterations in presynaptic number.

Physiologically, a reduction in release probability at PV-pyramidal cell synapses could result in decreased PV-pyramidal cell functional connectivity. Therefore, we measured release probability at PV-pyramidal cell synapses by recording the le-IPSC amplitudes evoked by four 5-ms pulses of blue light delivered at 20 Hz while holding pyramidal cells in the PrL mPFC of MIA and Saline offspring on a PV-ChR2 background at a membrane potential of −70 mV. Although for this analysis we only included cells where we were able to detect a significant le-IPSC, we still found an overall reduction in the le-IPSC amplitude in MIA offspring (Figure 3I; Stim 1: Saline, 72.93±13.04 pA; MIA, 40.67±15.80 pA; Stim 2: Saline, 28.18±5.35 pA; MIA, 19.50±7.18 pA; Stim 3: Saline, 19.16±3.86 pA; MIA, 14.30±5.02 pA; Stim 4: Saline, 14.22±2.11 pA; MIA, 8.19±3.29 pA; n=10 cells from 4 Saline offspring and 7 cells from 3 MIA offspring; 2-way repeated measures ANOVA: effect of treatment, $p<0.05$). We found that PV-pyramidal cell synapses in MIA offspring exhibited reduced paired-pulse depression relative to synapses in Saline offspring (Figure 3J; Stim 2 (% of Stim 1): Saline, 41.39±5.75; MIA, 60.40±8.78; Stim 3 (% of Stim 1): Saline, 27.53±3.20; MIA, 58.10±16.44; Stim 4 (% of Stim 1): Saline, 22.41±3.62; MIA, 37.05±21.81; n=10 cells from 4 Saline offspring and 7 cells from 3 MIA offspring; 2-way repeated measures ANOVA: effect of treatment, $p<0.05$), in line with decreased release probability. Decreased release probability would result in a loss of functional GABAergic transmission, and therefore potentially underlies the PV functional phenotype in the MIA offspring.

One mechanism contributing to release probability is the amount of presynaptic GABA available for release. The GABA-synthesizing enzyme, GAD67, regulates the production of GABA[53], and a reduction of GAD67 in PV cells has been shown to decrease both the frequency of spontaneous inhibitory currents in pyramidal cells of the prefrontal cortex[54] as well as the strength of GABAergic currents in pyramidal cells evoked by prefrontal electrical

stimulation[55]. Furthermore, GAD67 expression has been repeatedly shown to be reduced in the prefrontal cortex of post-mortem tissue from patients with schizophrenia[9, 11, 56-60], especially in PV-containing interneurons[10, 27]. Therefore, we measured GAD67 expression in PV interneurons in the PrL mPFC in adult MIA and Saline offspring. As GAD67 is expressed in both the cell soma as well as the presynaptic terminals, we chose to measure GAD67 in the clearly demarcated PV cell soma. We found a strong trend towards a reduction in the intensity of GAD67 staining in PV interneurons in adult MIA offspring (Figure 3K&L; GAD67 Mean Intensity (A.U.): Saline, 704.6±86.85, n=7; MIA, 518.2±37.32, n=7; t-test, p=0.07), suggesting that physiological changes in GABA synthesis may contribute to the deficit in GABAergic transmission from PV cells in MIA offspring.

To assess whether alterations in intrinsic excitability of PV interneurons contribute to this decrease in PV GABAergic transmission we measured active and passive membrane properties of PV cells in adult MIA and Saline offspring (Supplementary Figure S4). We found that the resting membrane potential, input resistance and sag ratio of PV cells was unchanged in MIA mice, but that their rheobase was decreased (Saline, 85.71±7.68 pA, n=14; MIA, 59.44±5.57, n=18; t-test, $p<0.01$) and their firing frequency as a function of input current was increased (2-way ANOVA, treatment by input current interaction, $p<0.001$), suggesting they are more excitable. Rather than contributing to decreased GABAergic transmission from PV cells, this change may reflect a compensatory alteration in the cells to accommodate for their decreased release probability (or vice versa).

Adult MIA offspring have intact spatial working memory but impaired attentional set shifting and increased anxiety levels

Due to the hypothesized role of prefrontal PV interneuron function in working memory, we investigated whether adult MIA offspring show deficits in working memory tasks. We found that adult MIA offspring do not show impairments in either the delayed non-match to sample (DNMS) t-maze task (Figure 4A-C), or an operant delayed alternation task (ODAT; Figure 4D-G), both of which probe working memory. In the DNMS t-maze, MIA and Saline offspring acquired the task equivalently, reaching performance criterion of 70% accuracy on 3 consecutive days within 7 days (Figure 4B; Saline, n=8 animals; MIA, n=9 animals). For all mice, performance decreased with increasing intra-trial delays, but MIA and Saline offspring performed equivalently (Figure 4C). In the ODAT, we observed that MIA mice acquired the task faster than Saline offspring (Figure 4E; 2-way repeated measures ANOVA: trial day by treatment interaction, $p<0.05$, Saline, n=15 animals, MIA, n=18 animals). While accuracy for all mice decreased when the intra-trial delay was increased from 2s to 16s, Saline and MIA offspring performed equivalently at the 16s delay (Figure 4F). Similar to what was seen with initial task acquisition, MIA offspring acquired the task faster when the reward contingency was reversed (Figure 4G; 2-way repeated measures ANOVA: effect of treatment, $p<0.01$).

Recent work has established a role for prefrontal GABAergic interneurons in governing attentional set shifting, another prefrontal-dependent cognitive task that is also impaired in patients with schizophrenia[37, 61]. MIA and Saline mice reached criterion in the initial acquisition (IA) portion of the task in a comparable number of trials (Figure 4I; Saline,

16.63±1.76 trials, n=8; MIA, 18.11±2.29 trials, n=9). However, in the set shifting (SS) portion of the task the Saline mice reached criterion in a significantly shorter number of trials than the MIA mice (Figure 4J; Saline, 11.43±0.72 trials, n=7; MIA, 18.75±2.34 trials, n=8; t-test, $p<0.05$; Note, 1 Saline and 1 MIA animal who completed the IA portion of the task did not complete the SS portion because of a loss of motivation to retrieve the rewards).

A role for prefrontal GABAergic interneurons in affective behaviors has also been hypothesized[62]. In keeping with this, we found that adult MIA offspring showed enhanced anxiety-related behavior (Figure 4K-M). Adult MIA offspring spend significantly less time in the anxiogenic open arms relative to the anxiolytic closed arms in the Elevated Plus Maze (EPM). The Open-Closed Arm Time Ratio for all mice was normalized to the Saline average (Normalized Open-Closed Arm Time Ratio; Figure 4L; Saline, 1.00±0.52, n=15 animals; MIA, 0.14±0.02, n=18 animals; Mann Whitney: $p<0.05$) in the EPM to facilitate comparison with the optogenetic experiments where it was necessary to normalize to compare results from two days of repeated maze testing (see below). The total distance traveled by the mice was unchanged (Figure 4M; Saline, 5.70±0.50 m; MIA, 6.31±0.46 m).

We verified the anxiety-like phenotype in the MIA offspring by using the open field task. MIA offspring spent significantly less time and distance in the center of the open field relative to the periphery as an indication of enhanced anxiety (Supplementary Figure S5A for time; Saline, 0.16±0.01, n=15; MIA, 0.11±0.01, n=18; t-test, $p<0.01$; Supplementary Figure S5B for distance; Saline, 0.28 ± 0.02, n=15; MIA, 0.21 ± 0.015, n=18; t-test, $p<0.01$).

Optogenetically silencing prefrontal PV interneurons impairs attentional set shifting and increases anxiety-related behaviors

To determine if impaired GABAergic transmission from prefrontal PV interneurons is sufficient to impair attentional set shifting and induce anxiety-related behaviors, we bilaterally injected the mPFC of PV-Cre mice with a virus that expresses the hyperpolarizing light-gated proton pump, eArch3.0, in a Cre-dependent manner (AAV5-ef1α-DIO-eArch3.0; AP +1.8, ML ±0.3, DV −1.8). We bilaterally implanted the mPFC with optical fibers (AP +1.8, ML ±0.3, DV −1.2) and decreased mPFC PV interneuron activity during behavior using green light stimulation. Control mice were injected with a comparable GFP-expressing virus (AAV5-hSYN-DIO-GFP). In the set shifting task, all mice performed the IA portion with the light OFF. Directly following IA, half the mice were randomized to have the light ON during the SS portion of the task and half the mice to have the light OFF. On the next day, the animals received IA followed by a second version of the SS task counterbalanced for the light condition (Figure 5A). The number of trials it took each animal to reach criterion for the SS portion of the task was compared when they had the light ON versus OFF. A comparison of the PV-GFP and PV-eArch3.0 mice in the set shifting portion of the task under light ON and OFF conditions using a 2-way repeated measures ANOVA revealed a significant effect of virus treatment (Figure 5B. PV-GFP OFF, 10.83±0.75 trials, n=6; PV-GFP ON, 11.67±1.50 trials, n=6; PV-eArch3.0 OFF, 12.78±1.50 trials, n=9; PV-eArch3.0 ON, 18.22±2.08 trials, n=9; 2-way repeated measures ANOVA, effect of virus, $p<0.05$). A

subsequent post-hoc comparison indicated that the PV-eArch3.0 ON group took significantly longer to complete the task than the PV-eArch3.0 OFF group (t-test, $p<0.05$).

We then tested the effects of inhibiting PV interneurons in the EPM task. Animals were tested twice, on two separate days, once with the light ON and once with it OFF, in a randomized, counter-balanced fashion. Time in the open arms relative to the closed arms was less for all animals on the second day of testing, possibly due to habituation to novelty occurring upon repeated maze exposure. Therefore, the Open-Closed Arm Time Ratio for each animal on a given day was normalized to the mean of the GFP light-OFF group on that day to yield a Normalized Open-Close Arm Time Ratio so that all animals could be analyzed under light ON and OFF conditions. PV-eArch3.0 mice had a significantly reduced Normalized Open-Close Arm Time Ratio in the EPM when the light was ON relative to when it was OFF and this effect was not seen in PV-GFP control mice (Figure 5D; PV-GFP OFF 1.00±0.43, n=10 animals PV-GFP ON, 1.37±0.52, n=10 animals; PV-eArch3.0 OFF, 0.92±0.15, n=17 animals; PV-eArch3.0 ON, 0.45±0.09, n=17 animals; 2-way repeated measures ANOVA: light by virus interaction $p<0.05$; paired t-test: PV-eArch3.0 Light ON versus Light OFF, $p<0.05$). This effect was not due to an overall change in movement as optogenetic suppression of PV activity did not impact the total distance traveled (Figure 5E; PV-GFP Light OFF, 4.35±0.46 m, n=10 animals; PV-GFP Light ON, 4.23±0.70 m, n=10 animals; PV-eArch3.0 Light ON, 5.46±0.40 m, n=17 animals; PV-eArch3.0 Light OFF, 5.74±0.45 m, n=17 animals) in the EPM.

Gamma power correlates with anxiety measures in control mice and this correlation is disrupted in MIA offspring

As PV interneuron function has been causally linked to gamma oscillations[32, 34], we measured oscillatory activity in the mPFC in mice performing the elevated plus maze test. We found that overall mean gamma power (30-80 Hz) was not significantly reduced in adult MIA offspring relative to Saline offspring in the EPM (Figure 5F; Saline, 4.7×10^{-11}±0.6×10^{-11} V^2/Hz, n=5; MIA, 3.5×10^{-11}±0.6×10^{-11} V^2/Hz, n=8; t-test, p=0.19). Strikingly, there was a strong relationship between the power of gamma oscillations and anxiety levels in the elevated plus maze in Saline mice (Figure 5G). Higher gamma power was correlated with increased open arm time in a linear fashion (Figure 5G; $r^2=0.84$, $p<0.05$, n=5). We subsequently confirmed this correlation in a larger independent dataset of 129SvEvTac mice (Supplementary Figure S6A; $r^2=0.53$ $p<0.01$, n=12). Gamma power was not different in the open versus closed arms (Supplementary Figure S6B; mean gamma in open, $1.73\pm0.18 \times 10^{-9}$ V^2/Hz; mean gamma in closed, $1.77\pm0.19 \times 10^{-9}$ V^2/Hz; n=12), demonstrating that the correlation is not simply a spurious consequence of the difference in time spent in the open arms. Notably, this correlation was disrupted in adult MIA offspring (Figure 5G; $r^2=0.02$, p=0.71, n=8). The correlation in MIA offspring remained non-significant with an r^2 value lower than that of Saline mice, even following removal of the MIA mouse whose data fell furthest from the best-fit line (Supplementary Figure S7).

Discussion

Histological studies of schizophrenia, bipolar disorder and depression have demonstrated abnormalities in interneurons that express the marker PV, while a non-overlapping population that expresses the marker CR does not appear affected[1, 10, 17, 19, 28-29, 38-40, 63]. Despite these changes at the protein and mRNA levels it is unclear whether GABAergic transmission is altered in the PFC in these disorders, and if so, whether the functional changes are restricted to particular interneuron subpopulations.

Using optogenetics combined with slice electrophysiology, we provide evidence that in an established risk factor model, the MIA model, GABAergic transmission is reduced in the mPFC. This reduction is due to a selective decrease in functional connectivity between the PV class of interneurons and pyramidal cells, while transmission from CR and SST interneurons to pyramidal neurons remains unaffected.

These cell-type specific functional changes in GABA transmission from PV interneurons were observed in the absence of any alterations in the number of PV-expressing cells or the number of PV or GAD65-positive perisomatic synapses. This suggests that these functional changes are not due to changes in PV cell number or anatomical connectivity. In contrast with the lack of anatomical changes, functional assessment of PV-pyramidal cell synapses indicates that presynaptic release probability is reduced in adult MIA offspring. Additionally, we observed a strong trend for GAD67 levels to be reduced in PV interneurons in the mPFC of adult MIA offspring. GAD67 regulates GABA production[53], and microRNA mediated as well as genetic reduction of GAD67 expression in PV interneurons has been shown to decrease GABA release[54-55]. Decreased GAD67 levels may therefore provide a mechanism to explain the reduction in functional GABAergic connectivity and release probability we observed in PV cells in the mPFC of adult MIA offspring. Moreover, this reduction in GAD67 in PV interneurons is consistent with what has been observed in histological studies of the PFC from patients with schizophrenia, where expression of GAD67 has been repeatedly shown to be reduced [9, 11, 56-60], especially in PV-containing interneurons[10, 27]. Cumulatively, our functional and histological studies in the MIA model indicate that interneuron function can be compromised under pathological conditions, in the absence of anatomical alterations.

Previous work using a higher dose of Poly IC (5 versus 1 mg/kg) and looking at older animals (six versus three-month old mice) found a decrease in histologically identified PV interneurons in the mPFC in adult MIA offspring[47]. The difference between these results and ours may stem from the different doses used or the age at which the brains were assessed. For example, it is possible that impairments of PV functional transmission may be at an earlier state in the disease process occurring before alterations in PV manifest histologically. While we cannot rule out the possibility that our histological methods were not sensitive enough to detect subtle differences in PV synapse number, our findings are consistent with those from the schizophrenia post-mortem literature where the number of PV/GAD65 double-labeled perisomatic puncta were unchanged in the PFC of patients[64].

Abnormalities in cortical PV interneurons have been extensively discussed in the context of cognitive deficits in schizophrenia, which include impairments in attentional set shifting and working memory[3, 61, 65-66]. Animal studies have demonstrated the role of PV interneurons in generating gamma oscillations[30, 32-34], which have in turn been shown to be important for attentional set shifting in mice[37] and to correlate with working memory performance in humans[36].

We found that adult MIA offspring show a deficit in attentional set shifting but not in another form of behavioral flexibility, reversal learning, which was actually was enhanced. This finding is consistent with findings by Cho et al, who used optogenetic tools to demonstrate the importance of medial prefrontal GABAergic interneurons for attentional set shifting, but not for reversal learning[37]. Our optogenetic inhibition experiments show that this holds true not only after pan-interneuronal inhibition of mPFC interneurons but also after selective inhibition of PV-interneurons. We therefore conclude that the decrease in PV GABAergic transmission observed in MIA offspring could be causally involved in generating the attentional set shifting deficit. Why reversal learning is enhanced in MIA offspring is currently unclear. Reversal learning is typically associated with serotonergic and dopaminergic signaling in the orbitofrontal cortex and dopaminergic signaling in the striatum and alterations in these systems in MIA mice may underlie the enhancement in reversal learning[67-72].

Despite the strong reduction in GABAergic transmission from PV inhibitory interneurons in the prefrontal cortex in MIA offspring, we did not observe any impairment in two independent prefrontal-dependent working memory tasks, the DNMS t-maze task, and an operant delayed alternation task[69, 73]. Although surprising in light of the hypothesized relationship between prefrontal PV interneurons and working memory[3], this result is consistent with the findings from other groups demonstrating that MIA in mid- (e12) or early- (e9) gestation is not associated with later working memory impairments[47, 74]. In contrast, MIA during late (e17) gestation has been found to impair working memory[47, 75-77]. A dissociation between reduced PV interneuron number and working memory impairments was also found in a study that utilized a higher dose of Poly IC (5 mg/kg) than used here. Although this dose of PolyIC produced histological deficits in mPFC PV interneurons in adult MIA offspring when it was administered at e9 or e17, working memory impairments were only seen at e17[47].

Our *in vivo* LFP recordings did not reveal a significant change in gamma frequency oscillations (30-80 Hz) in the mPFC of MIA offspring. As gamma frequency oscillations are known to be supported by PV interneuron function[32, 34], this finding was surprising. We may, however, not have detected changes in gamma power in MIA offspring because of homeostatic compensatory changes in PV interneurons, such as the observed increase in PV interneuron excitability. Although both attentional set shifting and working memory are thought to depend on task-induced gamma oscillations[3, 37, 78], so far this has only been shown directly for attentional set shifting[37]. Whether task induced gamma is altered during working memory or attentional set shifting in MIA offspring will need to be addressed with future experiments.

Alterations in prefrontal GABAergic transmission have also been hypothesized to underlie affective symptoms, such as enhanced anxiety[7, 62, 79-80]. Indeed, benzodiazepines have been used as adjunct therapy to treat anxiety in psychosis[81] and recent functional magnetic resonance imaging (fMRI) work suggests the PFC of patients with schizophrenia is differentially activated by benzodiazepine challenge during affective processing[62]. While healthy controls show decreased PFC activity compared to baseline when administered benzodiazepines, patients with schizophrenia exhibit a non-intuitive increase in PFC activity[62]. Similarly, in depression, decreased prefrontal GABA correlated with measures of anhedonia, and decreased GABA levels in the cerebral spinal fluid were associated with increased severity of anxiety, but not depressive, symptoms[7, 79]. Despite these intriguing clinical findings, relatively little preclinical work has examined a relationship between prefrontal GABAergic circuits and control of affective behaviors like anxiety.

We now provide several lines of evidence to suggest that GABAergic transmission from prefrontal PV interneurons is important for anxiety-like behavior. First, MIA offspring, who have a deficit in prefrontal GABAergic transmission, show increased anxiety-related behaviors. This finding is consistent with results from other groups using MIA models, which have found increased anxiety in adult MIA offspring[49, 82-87]. Second, optogenetically silencing prefrontal PV interneurons increases anxiety-like behavior. This result relates to a recent finding that this interneuron population plays an important role in the regulation of fear expression in cue-induced fear conditioning. Using an optogenetic approach similar to our own, Courtin et al demonstrated that mPFC PV interneurons are required for normal fear extinction in a fear conditioning paradigm[88]. While learned fear and innate anxiety are separate behavioral constructs, it is intriguing that both findings suggest that mPFC PV interneuron activity serves to suppress fear and anxiety. These results support a hypothesis proposed by Taylor and Welsh (2013) that prefrontal GABAergic abnormalities may be important for affective disturbances in psychiatric disorders[7, 62, 79-80].

In further support of a link between PV interneurons and anxiety-related behaviors, we found that gamma oscillations—a neurophysiological phenomenon that is known to depend on PV interneuron function—are significantly correlated with anxiety-like behavior as measured in the EPM in adult mice. In contrast, in MIA offspring, the linear correlation between gamma and anxiety-like behavior was disrupted. Our findings are interesting in the context of other studies that showed impaired long-range neural synchrony between hippocampus and mPFC in MIA offspring[89-90], which may contribute to the anxiety and set shifting phenotypes observed here.

At this point it is unclear how prenatal MIA leads to the impairment in PV GABAergic transmission in adult MIA offspring. The high metabolic demand that makes fast spiking PV interneurons particularly susceptible to oxidative stress may contribute to this effect[91-93]. Whether specific PV interneuron subtypes, such as chandelier versus basket cells, are differentially functionally altered in MIA offspring remains unknown, but is an intriguing question given that these different cell types may have potentially opposing functional effects on pyramidal cells[94-95]. Future studies could address this question using genetic tools that selectively target chandelier neurons[96].

In conclusion, this work provides evidence that the function of PV interneurons is particularly vulnerable to MIA. MIA can lead to a decreased release probability at PV interneuron-pyramidal cell synapses suggesting that a latent functional PV interneuron deficit can be present even before the deficit manifests histologically. Decreased PV to pyramidal neuron functional connectivity is sufficient to cause deficits in attentional set shifting and enhance anxiety-related behavior. We would suggest that this vulnerability circuit may also be affected in human offspring of mothers that were exposed to infections during pregnancy, with consequences for cognitive and affective behaviors. In support of this, schizophrenia patients with serological evidence of maternal infection during pregnancy performed more poorly on a test of set shifting behavior than those patients without evidence of maternal infection[61]. Our work suggests similar associations may exist for anxiety-related behaviors, which should be investigated in future epidemiological studies. Such deficits in specific cognitive and affective symptoms in schizophrenia as well as bipolar disorder may result from similar mechanisms as those described here.

Supplementary Material

Refer to Web version on PubMed Central for supplementary material.

Acknowledgments

We would like to thank Bhavani Ramesh, Mariya Shegda and Lindsay Kenney for their assistance with genotyping of mice and Heather Perusini, Kafi Friday and Katherine Yao for their assistance with behavioral and electrophysiological studies. Confocal images were collected in the Confocal and Specialized Microscopy Shared Resource of the Herbert Irving Comprehensive Cancer Center at Columbia University, supported by NIH grant #P30 CA013696 (National Cancer Institute). This work was supported by a Schaefer Research Scholar Award (CK), a NIMH T32 Training Grant (MH16434-31, SEC), NARSAD Young Investigator Award (SEC), a Sackler Institute for Developmental Psychobiology Fellowship (SEC), a K02 MH065422 (AB), and AA 19801 to NLH.

References

1. Sibille E, Morris HM, Kota RS, Lewis DA. GABA-related transcripts in the dorsolateral prefrontal cortex in mood disorders. Int J Neuropsychopharmacol. 2011; 14(6):721–734. [PubMed: 21226980]
2. Karolewicz B, Maciag D, O'Dwyer G, Stockmeier CA, Feyissa AM, Rajkowska G. Reduced level of glutamic acid decarboxylase-67 kDa in the prefrontal cortex in major depression. Int J Neuropsychopharmacol. 2010; 13(4):411–420. [PubMed: 20236554]
3. Lewis DA, Curley AA, Glausier JR, Volk DW. Cortical parvalbumin interneurons and cognitive dysfunction in schizophrenia. Trends Neurosci. 2012; 35(1):57–67. [PubMed: 22154068]
4. Sanacora G, Gueorguieva R, Epperson CN, Wu YT, Appel M, Rothman DL, et al. Subtype-specific alterations of gamma-aminobutyric acid and glutamate in patients with major depression. Arch Gen Psychiatry. 2004; 61(7):705–713. [PubMed: 15237082]
5. Sanacora G, Mason GF, Rothman DL, Behar KL, Hyder F, Petroff OA, et al. Reduced cortical gamma-aminobutyric acid levels in depressed patients determined by proton magnetic resonance spectroscopy. Arch Gen Psychiatry. 1999; 56(11):1043–1047. [PubMed: 10565505]
6. Bhagwagar Z, Wylezinska M, Jezzard P, Evans J, Ashworth F, Sule A, et al. Reduction in occipital cortex gamma-aminobutyric acid concentrations in medication-free recovered unipolar depressed and bipolar subjects. Biol Psychiatry. 2007; 61(6):806–812. [PubMed: 17210135]
7. Gabbay V, Mao X, Klein RG, Ely BA, Babb JS, Panzer AM, et al. Anterior cingulate cortex gamma-aminobutyric acid in depressed adolescents: relationship to anhedonia. Arch Gen Psychiatry. 2012; 69(2):139–149. [PubMed: 21969419]
8. Hasler G, van der Veen JW, Tumonis T, Meyers N, Shen J, Drevets WC. Reduced prefrontal glutamate/glutamine and gamma-aminobutyric acid levels in major depression determined using

proton magnetic resonance spectroscopy. Arch Gen Psychiatry. 2007; 64(2):193–200. [PubMed: 17283286]

9. Akbarian S, Kim JJ, Potkin SG, Hagman JO, Tafazzoli A, Bunney WE Jr, et al. Gene expression for glutamic acid decarboxylase is reduced without loss of neurons in prefrontal cortex of schizophrenics. Arch Gen Psychiatry. 1995; 52(4):258–266. [PubMed: 7702443]
10. Hashimoto T, Volk DW, Eggan SM, Mirnics K, Pierri JN, Sun Z, et al. Gene expression deficits in a subclass of GABA neurons in the prefrontal cortex of subjects with schizophrenia. J Neurosci. 2003; 23(15):6315–6326. [PubMed: 12867516]
11. Volk DW, Austin MC, Pierri JN, Sampson AR, Lewis DA. Decreased glutamic acid decarboxylase67 messenger RNA expression in a subset of prefrontal cortical gamma-aminobutyric acid neurons in subjects with schizophrenia. Arch Gen Psychiatry. 2000; 57(3):237–245. [PubMed: 10711910]
12. Schmidt MJ, Mirnics K. Neurodevelopment, GABA system dysfunction, and schizophrenia. Neuropsychopharmacology. 2015; 40(1):190–206. [PubMed: 24759129]
13. Frankle WG, Cho RY, Prasad KM, Mason NS, Paris J, Himes ML, et al. In Vivo Measurement of GABA Transmission in Healthy Subjects and Schizophrenia Patients. Am J Psychiatry. 2015 appiajp201514081031.
14. Mohler H. The GABA system in anxiety and depression and its therapeutic potential. Neuropharmacology. 2012; 62(1):42–53. [PubMed: 21889518]
15. Hasler G, Nugent AC, Carlson PJ, Carson RE, Geraci M, Drevets WC. Altered cerebral gamma-aminobutyric acid type A-benzodiazepine receptor binding in panic disorder determined by [11C]flumazenil positron emission tomography. Arch Gen Psychiatry. 2008; 65(10):1166–1175. [PubMed: 18838633]
16. Malizia AL, Cunningham VJ, Bell CJ, Liddle PF, Jones T, Nutt DJ. Decreased brain GABA(A)-benzodiazepine receptor binding in panic disorder: preliminary results from a quantitative PET study. Arch Gen Psychiatry. 1998; 55(8):715–720. [PubMed: 9707382]
17. Hoftman GD, Volk DW, Bazmi HH, Li S, Sampson AR, Lewis DA. Altered Cortical Expression of GABA-Related Genes in Schizophrenia: Illness Progression vs Developmental Disturbance. Schizophr Bull. 2013
18. Hashimoto T, Arion D, Unger T, Maldonado-Aviles JG, Morris HM, Volk DW, et al. Alterations in GABA-related transcriptome in the dorsolateral prefrontal cortex of subjects with schizophrenia. Mol Psychiatry. 2008; 13(2):147–161. [PubMed: 17471287]
19. Hashimoto T, Bazmi HH, Mirnics K, Wu Q, Sampson AR, Lewis DA. Conserved regional patterns of GABA-related transcript expression in the neocortex of subjects with schizophrenia. Am J Psychiatry. 2008; 165(4):479–489. [PubMed: 18281411]
20. Maldonado-Aviles JG, Curley AA, Hashimoto T, Morrow AL, Ramsey AJ, O'Donnell P, et al. Altered markers of tonic inhibition in the dorsolateral prefrontal cortex of subjects with schizophrenia. Am J Psychiatry. 2009; 166(4):450–459. [PubMed: 19289452]
21. Beneyto M, Abbott A, Hashimoto T, Lewis DA. Lamina-specific alterations in cortical GABA(A) receptor subunit expression in schizophrenia. Cereb Cortex. 2011; 21(5):999–1011. [PubMed: 20843900]
22. Kegeles LS, Mao X, Stanford AD, Girgis R, Ojeil N, Xu X, et al. Elevated prefrontal cortex gamma-aminobutyric acid and glutamate-glutamine levels in schizophrenia measured in vivo with proton magnetic resonance spectroscopy. Arch Gen Psychiatry. 2012; 69(5):449–459. [PubMed: 22213769]
23. Markram H, Toledo-Rodriguez M, Wang Y, Gupta A, Silberberg G, Wu C. Interneurons of the neocortical inhibitory system. Nat Rev Neurosci. 2004; 5(10):793–807. [PubMed: 15378039]
24. Kepecs A, Fishell G. Interneuron cell types are fit to function. Nature. 2014; 505(7483):318–326. [PubMed: 24429630]
25. Wonders CP, Anderson SA. The origin and specification of cortical interneurons. Nat Rev Neurosci. 2006; 7(9):687–696. [PubMed: 16883309]
26. Fung SJ, Webster MJ, Sivagnanasundaram S, Duncan C, Elashoff M, Weickert CS. Expression of interneuron markers in the dorsolateral prefrontal cortex of the developing human and in schizophrenia. Am J Psychiatry. 2010; 167(12):1479–1488. [PubMed: 21041246]

27. Curley AA, Arion D, Volk DW, Asafu-Adjei JK, Sampson AR, Fish KN, et al. Cortical deficits of glutamic acid decarboxylase 67 expression in schizophrenia: clinical, protein, and cell type-specific features. Am J Psychiatry. 2011; 168(9):921–929. [PubMed: 21632647]
28. Khundakar A, Morris C, Thomas AJ. The immunohistochemical examination of GABAergic interneuron markers in the dorsolateral prefrontal cortex of patients with late-life depression. Int Psychogeriatr. 2011; 23(4):644–653. [PubMed: 21044398]
29. Torrey EF, Barci BM, Webster MJ, Bartko JJ, Meador-Woodruff JH, Knable MB. Neurochemical markers for schizophrenia, bipolar disorder, and major depression in postmortem brains. Biol Psychiatry. 2005; 57(3):252–260. [PubMed: 15691526]
30. Bartos M, Vida I, Jonas P. Synaptic mechanisms of synchronized gamma oscillations in inhibitory interneuron networks. Nat Rev Neurosci. 2007; 8(1):45–56. [PubMed: 17180162]
31. Bressler SL, Freeman WJ. Frequency analysis of olfactory system EEG in cat, rabbit, and rat. Electroencephalogr Clin Neurophysiol. 1980; 50(1-2):19–24. [PubMed: 6159187]
32. Cardin JA, Carlen M, Meletis K, Knoblich U, Zhang F, Deisseroth K, et al. Driving fast-spiking cells induces gamma rhythm and controls sensory responses. Nature. 2009; 459(7247):663–667. [PubMed: 19396156]
33. Fuchs EC, Zivkovic AR, Cunningham MO, Middleton S, Lebeau FE, Bannerman DM, et al. Recruitment of parvalbumin-positive interneurons determines hippocampal function and associated behavior. Neuron. 2007; 53(4):591–604. [PubMed: 17296559]
34. Sohal VS, Zhang F, Yizhar O, Deisseroth K. Parvalbumin neurons and gamma rhythms enhance cortical circuit performance. Nature. 2009; 459(7247):698–702. [PubMed: 19396159]
35. Uhlhaas PJ, Singer W. Abnormal neural oscillations and synchrony in schizophrenia. Nat Rev Neurosci. 2010; 11(2):100–113. [PubMed: 20087360]
36. Tallon-Baudry C, Bertrand O, Peronnet F, Pernier J. Induced gamma-band activity during the delay of a visual short-term memory task in humans. J Neurosci. 1998; 18(11):4244–4254. [PubMed: 9592102]
37. Cho KK, Hoch R, Lee AT, Patel T, Rubenstein JL, Sohal VS. Gamma rhythms link prefrontal interneuron dysfunction with cognitive inflexibility in dlx5/6(+/−) mice. Neuron. 2015; 85(6): 1332–1343. [PubMed: 25754826]
38. Volk DW, Matsubara T, Li S, Sengupta EJ, Georgiev D, Minabe Y, et al. Deficits in transcriptional regulators of cortical parvalbumin neurons in schizophrenia. Am J Psychiatry. 2012; 169(10): 1082–1091. [PubMed: 22983435]
39. Cotter D, Landau S, Beasley C, Stevenson R, Chana G, MacMillan L, et al. The density and spatial distribution of GABAergic neurons, labelled using calcium binding proteins, in the anterior cingulate cortex in major depressive disorder, bipolar disorder, and schizophrenia. Biol Psychiatry. 2002; 51(5):377–386. [PubMed: 11904132]
40. Tooney PA, Chahl LA. Neurons expressing calcium-binding proteins in the prefrontal cortex in schizophrenia. Prog Neuropsychopharmacol Biol Psychiatry. 2004; 28(2):273–278. [PubMed: 14751422]
41. Brown AS, Derkits EJ. Prenatal infection and schizophrenia: a review of epidemiologic and translational studies. Am J Psychiatry. 2010; 167(3):261–280. [PubMed: 20123911]
42. Parboosing R, Bao Y, Shen L, Schaefer CA, Brown AS. Gestational influenza and bipolar disorder in adult offspring. JAMA Psychiatry. 2013; 70(7):677–685. [PubMed: 23699867]
43. Canetta SE, Bao Y, Co MD, Ennis FA, Cruz J, Terajima M, et al. Serological documentation of maternal influenza exposure and bipolar disorder in adult offspring. Am J Psychiatry. 2014; 171(5):557–563. [PubMed: 24480930]
44. Betts KS, Salom CL, Williams GM, Najman JM, Alati R. Associations between self-reported symptoms of prenatal maternal infection and post-traumatic stress disorder in offspring: evidence from a prospective birth cohort study. Journal of affective disorders. 2015; 175:241–247. [PubMed: 25658498]
45. Machon RA, Mednick SA, Huttunen MO. Adult major affective disorder after prenatal exposure to an influenza epidemic. Arch Gen Psychiatry. 1997; 54(4):322–328. [PubMed: 9107148]
46. Patterson PH. Immune involvement in schizophrenia and autism: etiology, pathology and animal models. Behav Brain Res. 2009; 204(2):313–321. [PubMed: 19136031]

47. Meyer U, Nyffeler M, Yee BK, Knuesel I, Feldon J. Adult brain and behavioral pathological markers of prenatal immune challenge during early/middle and late fetal development in mice. Brain Behav Immun. 2008; 22(4):469–486. [PubMed: 18023140]
48. Brown AS, Begg MD, Gravenstein S, Schaefer CA, Wyatt RJ, Bresnahan M, et al. Serologic evidence of prenatal influenza in the etiology of schizophrenia. Arch Gen Psychiatry. 2004; 61(8): 774–780. [PubMed: 15289276]
49. Meyer U, Nyffeler M, Engler A, Urwyler A, Schedlowski M, Knuesel I, et al. The time of prenatal immune challenge determines the specificity of inflammation-mediated brain and behavioral pathology. J Neurosci. 2006; 26(18):4752–4762. [PubMed: 16672647]
50. Pi HJ, Hangya B, Kvitsiani D, Sanders JI, Huang ZJ, Kepecs A. Cortical interneurons that specialize in disinhibitory control. Nature. 2013; 503(7477):521–524. [PubMed: 24097352]
51. Xu X, Roby KD, Callaway EM. Immunochemical characterization of inhibitory mouse cortical neurons: three chemically distinct classes of inhibitory cells. The Journal of comparative neurology. 2010; 518(3):389–404. [PubMed: 19950390]
52. Gabbott PL, Bacon SJ. Vasoactive intestinal polypeptide containing neurones in monkey medial prefrontal cortex (mPFC): colocalisation with calretinin. Brain Res. 1997; 744(1):179–184. [PubMed: 9030431]
53. Fenalti G, Law RH, Buckle AM, Langendorf C, Tuck K, Rosado CJ, et al. GABA production by glutamic acid decarboxylase is regulated by a dynamic catalytic loop. Nat Struct Mol Biol. 2007; 14(4):280–286. [PubMed: 17384644]
54. Brown JA, Ramikie TS, Schmidt MJ, Baldi R, Garbett K, Everheart MG, et al. Inhibition of parvalbumin-expressing interneurons results in complex behavioral changes. Mol Psychiatry. 2015
55. Fujihara K, Miwa H, Kakizaki T, Kaneko R, Mikuni M, Tanahira C, et al. Glutamate Decarboxylase 67 Deficiency in a Subset of GABAergic Neurons Induces Schizophrenia-Related Phenotypes. Neuropsychopharmacology. 2015; 40(10):2475–2486. [PubMed: 25904362]
56. Duncan CE, Webster MJ, Rothmond DA, Bahn S, Elashoff M, Shannon Weickert C. Prefrontal GABA(A) receptor alpha-subunit expression in normal postnatal human development and schizophrenia. J Psychiatr Res. 2010; 44(10):673–681. [PubMed: 20100621]
57. Hashimoto T, Bergen SE, Nguyen QL, Xu B, Monteggia LM, Pierri JN, et al. Relationship of brain-derived neurotrophic factor and its receptor TrkB to altered inhibitory prefrontal circuitry in schizophrenia. J Neurosci. 2005; 25(2):372–383. [PubMed: 15647480]
58. Thompson M, Weickert CS, Wyatt E, Webster MJ. Decreased glutamic acid decarboxylase(67) mRNA expression in multiple brain areas of patients with schizophrenia and mood disorders. J Psychiatr Res. 2009; 43(11):970–977. [PubMed: 19321177]
59. Woo TU, Kim AM, Viscidi E. Disease-specific alterations in glutamatergic neurotransmission on inhibitory interneurons in the prefrontal cortex in schizophrenia. Brain Res. 2008; 1218:267–277. [PubMed: 18534564]
60. Guidotti A, Auta J, Davis JM, Di-Giorgi-Gerevini V, Dwivedi Y, Grayson DR, et al. Decrease in reelin and glutamic acid decarboxylase67 (GAD67) expression in schizophrenia and bipolar disorder: a postmortem brain study. Arch Gen Psychiatry. 2000; 57(11):1061–1069. [PubMed: 11074872]
61. Brown AS, Vinogradov S, Kremen WS, Poole JH, Deicken RF, Penner JD, et al. Prenatal exposure to maternal infection and executive dysfunction in adult schizophrenia. Am J Psychiatry. 2009; 166(6):683–690. [PubMed: 19369317]
62. Taylor SF, Demeter E, Phan KL, Tso IF, Welsh RC. Abnormal GABAergic function and negative affect in schizophrenia. Neuropsychopharmacology. 2014; 39(4):1000–1008. [PubMed: 24154667]
63. Lewis DA, Hashimoto T, Volk DW. Cortical inhibitory neurons and schizophrenia. Nat Rev Neurosci. 2005; 6(4):312–324. [PubMed: 15803162]
64. Glausier JR, Fish KN, Lewis DA. Altered parvalbumin basket cell inputs in the dorsolateral prefrontal cortex of schizophrenia subjects. Mol Psychiatry. 2014; 19(1):30–36. [PubMed: 24217255]
65. Gonzalez-Burgos G, Fish KN, Lewis DA. GABA neuron alterations, cortical circuit dysfunction and cognitive deficits in schizophrenia. Neural plasticity. 2011; 2011:723184. [PubMed: 21904685]

66. Barch DM, Sheffield JM. Cognitive impairments in psychotic disorders: common mechanisms and measurement. World psychiatry : official journal of the World Psychiatric Association. 2014; 13(3):224–232.

67. Kehagia AA, Murray GK, Robbins TW. Learning and cognitive flexibility: frontostriatal function and monoaminergic modulation. Curr Opin Neurobiol. 2010; 20(2):199–204. [PubMed: 20167474]

68. Darvas M, Palmiter RD. Contributions of striatal dopamine signaling to the modulation of cognitive flexibility. Biol Psychiatry. 2011; 69(7):704–707. [PubMed: 21074144]

69. Rossi MA, Hayrapetyan VY, Maimon B, Mak K, Je HS, Yin HH. Prefrontal cortical mechanisms underlying delayed alternation in mice. J Neurophysiol. 2012; 108(4):1211–1222. [PubMed: 22539827]

70. Vuillermot S, Weber L, Feldon J, Meyer U. A longitudinal examination of the neurodevelopmental impact of prenatal immune activation in mice reveals primary defects in dopaminergic development relevant to schizophrenia. J Neurosci. 2010; 30(4):1270–1287. [PubMed: 20107055]

71. Winter C, Djodari-Irani A, Sohr R, Morgenstern R, Feldon J, Juckel G, et al. Prenatal immune activation leads to multiple changes in basal neurotransmitter levels in the adult brain: implications for brain disorders of neurodevelopmental origin such as schizophrenia. Int J Neuropsychopharmacol. 2009; 12(4):513–524. [PubMed: 18752727]

72. Mizoguchi K, Shoji H, Tanaka Y, Tabira T. Orbitofrontal dopaminergic dysfunction causes age-related impairment of reversal learning in rats. Neuroscience. 2010; 170(4):1110–1119. [PubMed: 20736050]

73. Kellendonk C, Simpson EH, Polan HJ, Malleret G, Vronskaya S, Winiger V, et al. Transient and selective overexpression of dopamine D2 receptors in the striatum causes persistent abnormalities in prefrontal cortex functioning. Neuron. 2006; 49(4):603–615. [PubMed: 16476668]

74. Connor CM, Dincer A, Straubhaar J, Galler JR, Houston IB, Akbarian S. Maternal immune activation alters behavior in adult offspring, with subtle changes in the cortical transcriptome and epigenome. Schizophr Res. 2012; 140(1-3):175–184. [PubMed: 22804924]

75. Richetto J, Calabrese F, Meyer U, Riva MA. Prenatal versus postnatal maternal factors in the development of infection-induced working memory impairments in mice. Brain Behav Immun. 2013; 33:190–200. [PubMed: 23876745]

76. Bitanihirwe BK, Weber L, Feldon J, Meyer U. Cognitive impairment following prenatal immune challenge in mice correlates with prefrontal cortical AKT1 deficiency. Int J Neuropsychopharmacol. 2010; 13(8):981–996. [PubMed: 20219156]

77. Kirwan CB, Gilbert PE, Kesner RP. The role of the hippocampus in the retrieval of a spatial location. Neurobiology of learning and memory. 2005; 83(1):65–71. [PubMed: 15607690]

78. Lewis DA. Inhibitory neurons in human cortical circuits: substrate for cognitive dysfunction in schizophrenia. Curr Opin Neurobiol. 2014; 26:22–26. [PubMed: 24650500]

79. Mann JJ, Oquendo MA, Watson KT, Boldrini M, Malone KM, Ellis SP, et al. Anxiety in major depression and cerebrospinal fluid free gamma-aminobutyric acid. Depress Anxiety. 2014; 31(10): 814–821. [PubMed: 24865448]

80. Altindag A, Yanik M, Nebioglu M. The comorbidity of anxiety disorders in bipolar I patients: prevalence and clinical correlates. Isr J Psychiatry Relat Sci. 2006; 43(1):10–15. [PubMed: 16910379]

81. Wassef AA, Dott SG, Harris A, Brown A, O'Boyle M, Meyer WJ 3rd, et al. Critical review of GABA-ergic drugs in the treatment of schizophrenia. Journal of clinical psychopharmacology. 1999; 19(3):222–232. [PubMed: 10350028]

82. Shi L, Fatemi SH, Sidwell RW, Patterson PH. Maternal influenza infection causes marked behavioral and pharmacological changes in the offspring. J Neurosci. 2003; 23(1):297–302. [PubMed: 12514227]

83. Yee N, Ribic A, de Roo CC, Fuchs E. Differential effects of maternal immune activation and juvenile stress on anxiety-like behaviour and physiology in adult rats: no evidence for the “double-hit hypothesis”. Behav Brain Res. 2011; 224(1):180–188. [PubMed: 21679729]

84. Lin YL, Wang S. Prenatal lipopolysaccharide exposure increases depression-like behaviors and reduces hippocampal neurogenesis in adult rats. Behav Brain Res. 2014; 259:24–34. [PubMed: 24177209]

85. Enayati M, Solati J, Hosseini MH, Shahi HR, Saki G, Salari AA. Maternal infection during late pregnancy increases anxiety- and depression-like behaviors with increasing age in male offspring. Brain research bulletin. 2012; 87(2-3):295–302. [PubMed: 21893170]

86. Hsiao EY, McBride SW, Chow J, Mazmanian SK, Patterson PH. Modeling an autism risk factor in mice leads to permanent immune dysregulation. Proc Natl Acad Sci U S A. 2012; 109(31):12776–12781. [PubMed: 22802640]

87. Smith SE, Li J, Garbett K, Mirnics K, Patterson PH. Maternal immune activation alters fetal brain development through interleukin-6. J Neurosci. 2007; 27(40):10695–10702. [PubMed: 17913903]

88. Courtin J, Chaudun F, Rozeske RR, Karalis N, Gonzalez-Campo C, Wurtz H, et al. Prefrontal parvalbumin interneurons shape neuronal activity to drive fear expression. Nature. 2014; 505(7481):92–96. [PubMed: 24256726]

89. Dickerson DD, Wolff AR, Bilkey DK. Abnormal long-range neural synchrony in a maternal immune activation animal model of schizophrenia. J Neurosci. 2010; 30(37):12424–12431. [PubMed: 20844137]

90. Dickerson DD, Overeem KA, Wolff AR, Williams JM, Abraham WC, Bilkey DK. Association of aberrant neural synchrony and altered GAD67 expression following exposure to maternal immune activation, a risk factor for schizophrenia. Translational psychiatry. 2014; 4:e418. [PubMed: 25072323]

91. Behrens MM, Sejnowski TJ. Does schizophrenia arise from oxidative dysregulation of parvalbumin-interneurons in the developing cortex? Neuropharmacology. 2009; 57(3):193–200. [PubMed: 19523965]

92. O'Donnell P. Cortical interneurons, immune factors and oxidative stress as early targets for schizophrenia. Eur J Neurosci. 2012; 35(12):1866–1870. [PubMed: 22708597]

93. Cabungcal JH, Steullet P, Kraftsik R, Cuenod M, Do KQ. Early-life insults impair parvalbumin interneurons via oxidative stress: reversal by N-acetylcysteine. Biol Psychiatry. 2013; 73(6):574–582. [PubMed: 23140664]

94. Woodruff A, Xu Q, Anderson SA, Yuste R. Depolarizing effect of neocortical chandelier neurons. Front Neural Circuits. 2009; 3:15. [PubMed: 19876404]

95. Glickfeld LL, Roberts JD, Somogyi P, Scanziani M. Interneurons hyperpolarize pyramidal cells along their entire somatodendritic axis. Nat Neurosci. 2009; 12(1):21–23. [PubMed: 19029887]

96. Taniguchi H, Lu J, Huang ZJ. The spatial and temporal origin of chandelier cells in mouse neocortex. Science. 2013; 339(6115):70–74. [PubMed: 23180771]

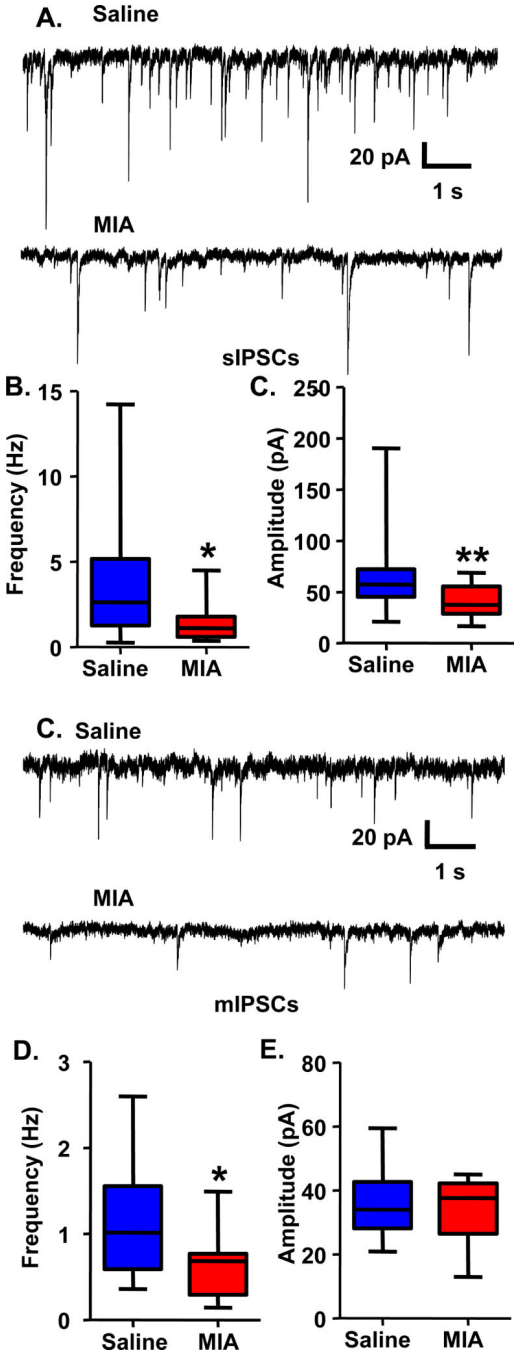

Figure 1.

Decreased sIPSC frequency and amplitude and mIPSC frequency in mPFC pyramidal cells from adult MIA offspring. (A) Example traces showing sIPSCs recorded using a KCl-based intracellular solution in gap-free mode at a holding potential of −70 mV from pyramidal cells from adult Saline or MIA offspring with 20 μM CNQX and 50 μM AP5 in the bath. (B) The frequency and amplitude of sIPSCs were decreased in MIA offspring. (C) Example traces showing mIPSCs recorded using a KCl-based intracellular solution in gap-free mode at a holding potential of −70 mV from pyramidal cells from adult Saline or MIA offspring

with 20 μM CNQX, 50 μM AP5 and 2 μM TTX in the bath. (D) The frequency, but not the amplitude, of mIPSCs was decreased in MIA offspring. *p<0.05.

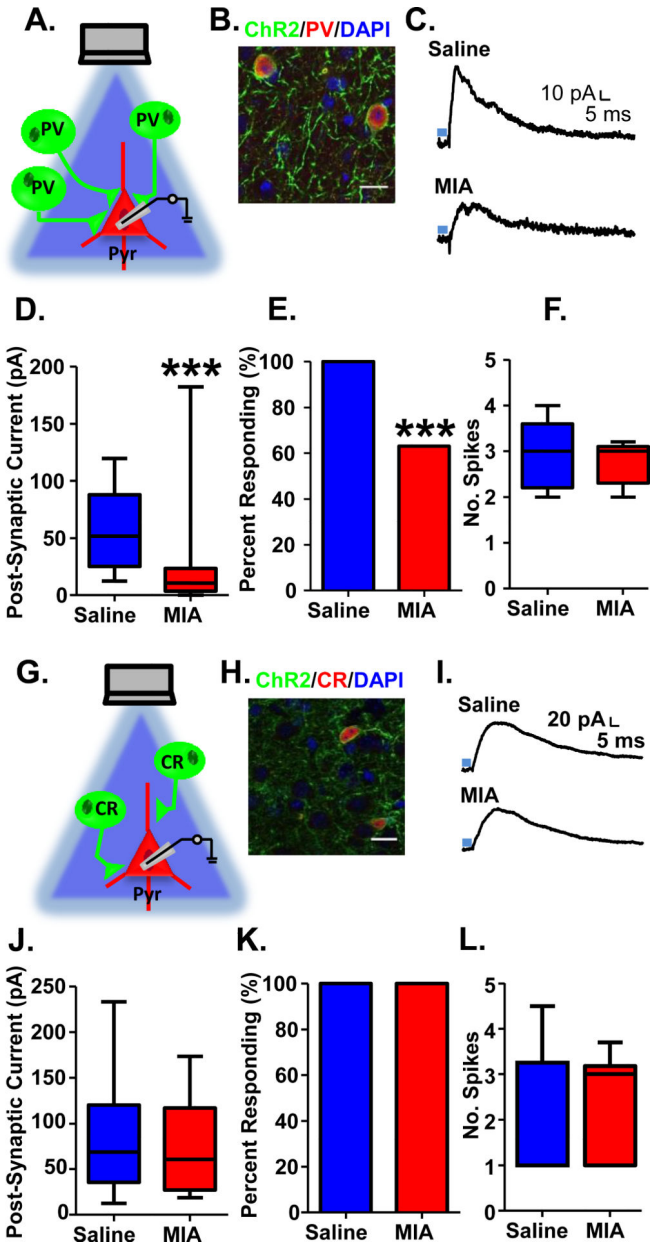

Figure 2.

Decreased light-evoked PV GABAergic transmission onto pyramidal cells in mPFC of adult MIA offspring. (A) Schematic illustrating experiment in PV-ChR2 mice. (B) ChR2-YFP (green) is expressed exclusively in PV interneurons (red; DAPI-labeled nuclei are shown in blue). (C) Example traces showing inhibitory post-synaptic currents (IPSCs) recorded in pyramidal cells from the mPFC of adult Saline and MIA offspring evoked by 5 ms stimulation with 470 nm blue light (blue bar) at a holding potential of −70 mV. (D) The amplitude of the light-evoked IPSCs as well as (E) the percent of pyramidal cells showing a significant light-evoked IPSC response was significantly decreased in the MIA offspring. (F) The number of spikes evoked by 5 ms of light-stimulation of ChR2-expressing PV cells in the mPFC of adult MIA offspring was unchanged. (G) Schematic illustrating experiment in

CR-ChR2 mice. (H) ChR2-YFP (green) is expressed exclusively in CR interneurons (red; DAPI-labeled nuclei are shown in blue). (I) Example traces showing inhibitory post-synaptic currents (IPSCs) recorded in pyramidal cells from the mPFC of adult Saline and MIA offspring evoked by 5 ms stimulation with 470 nm blue light (blue bar) in the presence of 20 μM CNQX and 50 μM AP5 at a holding potential of −50 mV. (J) The amplitude of the light-evoked IPSCs as well as (K) the percent of pyramidal cells showing a significant light-evoked IPSC response was unchanged in the MIA offspring. (L) The number of spikes evoked by 5 ms of light-stimulation of ChR2-expressing CR cells in the mPFC of adult MIA offspring was unchanged. ***$p<0.001$. Scale bar = 20 μm. (See also Supplementary Figure S1 and S2).

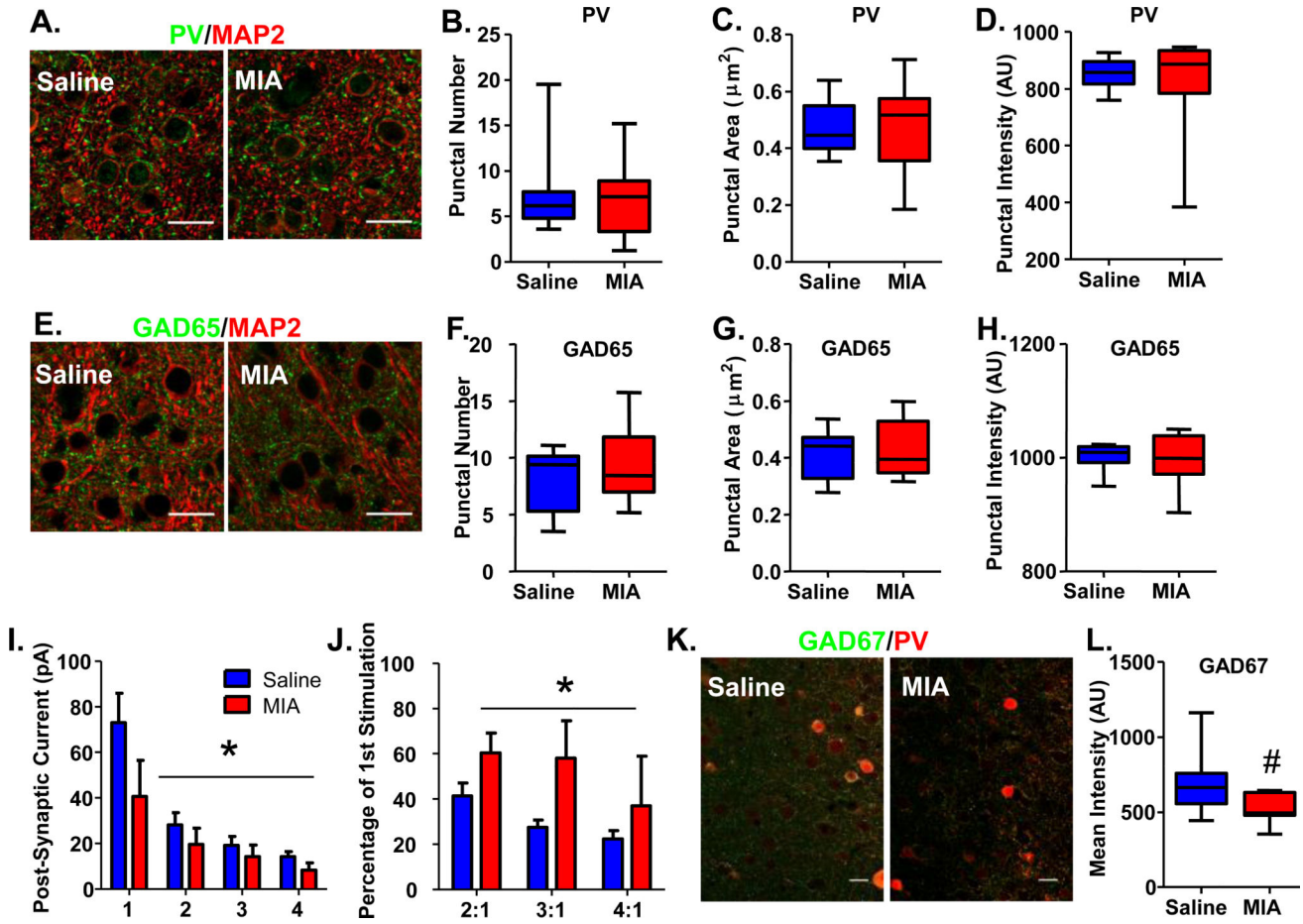

Figure 3.

GAD65 and PV perisomatic puncta are not altered, but presynaptic release probability and GAD67 expression is decreased in PV cells in the mPFC of adult MIA offspring. (A) Examples of PV/MAP2 staining of the mPFC of Saline and MIA offspring. (B) The number, (C) area and (D) intensity of PV-expressing perisomatic puncta surrounding pyramidal cells in the mPFC are unaltered in adult MIA offspring. (E) Examples of GAD65/MAP2 staining of the mPFC of Saline and MIA offspring. (F) The number, (G) area and (H) intensity of GAD65-expressing perisomatic puncta surrounding pyramidal cells in the mPFC are also unchanged in adult MIA offspring. (I) Four 5 ms pulses of blue light were delivered at 20 Hz to slices of mPFC from adult MIA or Saline offspring expressing ChR2 in PV cells. The amplitudes of the post-synaptic currents evoked in pyramidal cells by light stimulation were significantly smaller in MIA offspring. (J) The ratio of the amplitudes of the post-synaptic currents evoked in pyramidal cells by the 2nd, 3rd and 4th stimulation with light compared with the 1st stimulation were significantly increased in MIA offspring. (K) Examples of GAD67/PV staining of the mPFC of Saline and MIA offspring. (L) The mean intensity of GAD67 staining within PV cells exhibited a strong trend towards being decreased in MIA offspring. Scale bar = 20 μm. *$p<0.05$. $^{\#}p=0.07$. (See also Supplementary Figure S3 and S4).

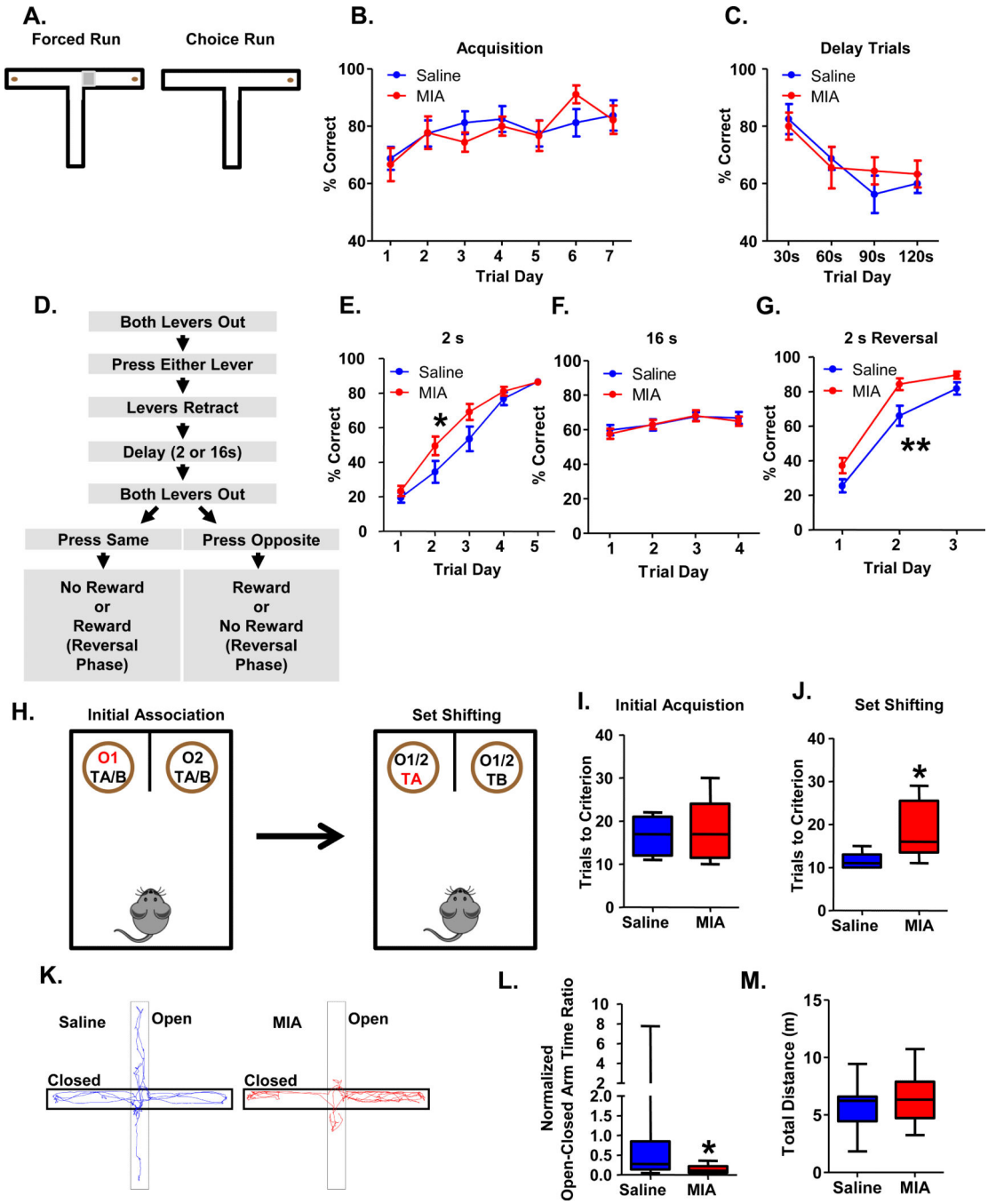

Figure 4.

Adult MIA offspring are not impaired in tests of working memory but show impairments in attentional set shifting and increased anxiety-related behaviors. (A) Diagram of the t-maze task. Each trial consisted of 2 runs. On the first run, mice are forced to either the left or the right arm, where they obtain a food reward. After a pre-determined delay, during the choice run, the mice are allowed to choose either arm, but only selection of the opposite arm results in a food reward. (B) Adult MIA offspring learn the t-maze task comparably to Saline offspring. (C) Adult MIA offspring perform comparably to Saline offspring as the working

memory load is increased in the t-maze task. (D) Flow chart of the delayed alternation task (see Supplemental Methods for details). (E) Adult MIA offspring acquire the delayed alternation task, using a 2 s intra-trial interval, more rapidly than Saline offspring (treatment by trial day interaction, *$p<0.05$). (F) Adult MIA offspring perform comparably when the working memory load is increased by increasing the intra-trial interval to 16s in the delayed alternation task. (G) Adult MIA offspring acquire the reversal rule faster than Saline offspring (**$p<0.01$, effect of treatment). (H) Diagram of the attentional set shifting task. In the initial acquisition phase, mice must learn to associate an odor with the presence of a reward, irrespective of the bedding medium that is present. Once the animal reaches criterion (8 of 10 consecutive correct trials), it proceeds to the set shifting portion of the task where the animal must now learn that the bedding medium predicts the presence of a reward irrespective of the odor. (I) MIA and Saline offspring acquire the task in an equivalent number of trials. (J) MIA offspring take significantly longer to reach criterion in the set shifting portion of the task. (K) Representative paths taken by MIA and Saline offspring in the Elevated Plus Maze. (L) MIA offspring spend significantly less time in the open arms of the EPM relative to the closed arms although (M) they travel an equivalent distance overall in the task. (See also Supplementary Figure S5).

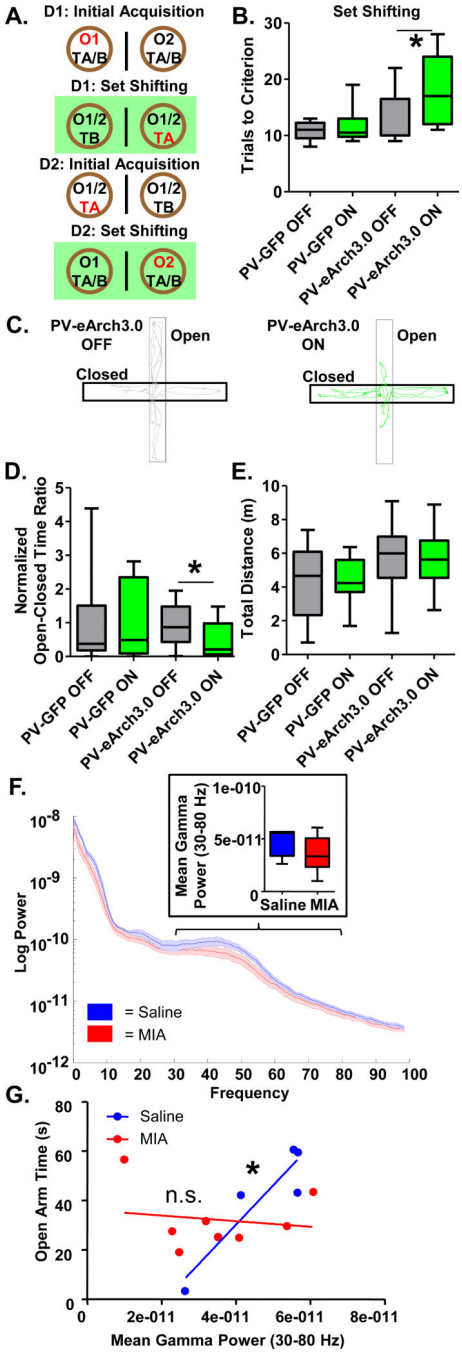

Figure 5.

mPFC PV interneuron dysfunction may mediate impaired attentional set shifting and increased innate anxiety-like behavior in adult MIA offspring. (A) Diagram of experimental set-up for the attentional set shifting task. Mice were tested on 2 consecutive days with the mice randomized to have the light ON during the set shifting portion of the task on the first day or the second day. (B) Mice expressing e-Arch3.0 in PV interneurons in the mPFC (PV-eArch3.0) require significantly more trials to complete the set shifting portion of the task when the light is ON then when it is OFF. Light has no effect on the mice expressing GFP in

PV interneurons in the mPFC (PV-GFP) control group. (C) Representative traces of the path taken by PV-eArch3.0 mice when the light is ON or OFF during the EPM. (D) The ratio of the time spent in the open arms relative to the closed arms (normalized to the GFP Light OFF average) is decreased in the PV-eArch3.0 mice when the light is ON, relative to when it's OFF, in the EPM. (E) Light has no effect on total distance traveled in the EPM. (F) Mean gamma power (30-80 Hz) in the mPFC of adult MIA offspring exploring the EPM is unchanged relative to Saline offspring. (G) In adult Saline offspring, but not adult MIA offspring, mean gamma power in the mPFC correlates with open arm time in the EPM. *$p<0.05$. (See also Supplementary Figures S6 and S7).

Table 1

Maternal serum cytokine response profile following injection of Poly IC or Saline.

	Saline	1 mg/kg Poly IC	2.5 mg/kg Poly IC	5 mg/kg Poly IC
IL-6 (pg/mL)	25±6	20405±4299	36430±4066***	155828±51107***
TNFα (pg/mL)	16±0	77±43	151±64	485±187**

Levels of interleukin-6 (IL-6) and tumor necrosis factor alpha (TNFα) were analyzed from serum collected from pregnant mothers 3 hours following an injection of 1, 2.5 or 5 mg/kg Poly IC or Saline on embryonic day 9. Poly IC dose-dependently increased maternal serum levels of both IL-6 and TNFα. Data shown is mean±standard error of the mean. N-values for IL-6 experiment are Saline (7), 1 mg/kg Poly IC (6), 2.5 mg/kg Poly IC (7), 5 mg/kg Poly IC (6). N-values for TNFα experiment are Saline (4), 1 mg/kg Poly IC (3), 2.5 mg/kg Poly IC (3), 5 mg/kg Poly IC (3). Kruskill-Wallis test followed by Dunn's Multiple Comparison test.

** $p<0.01$

*** $p<0.001$.

Table 2

Maternal and fetal outcomes following injection of Poly IC or Saline. Poly IC administered on embryonic day 9 dose-dependently increased maternal and fetal deaths.

Treatment	Injected	Maternal Deaths	Live Births	% Live Births	Surviving Pups	Male Pups	Female Pups	Pups Lost	Average Surviving Pups/Litter
Saline	5	0	5	100	21	13	8	7	4
1 mg/kg Poly IC	9	0	7	78	18	11	7	6	3
2.5 mg/kg Poly IC	7	0	2	29	5	1	4	1	3
5 mg/kg Poly IC	8	4	0	0					